Investigating the linkages between Indo-Pacific Ocean SST, Z_{500} climate variability and Tasmanian seasonal streamflow

M S Shams[1], A. H. M. F Anwar[1], K W Lamb[2]
[1]Department of Civil Engineering, Curtin University, Western Australia
[2]Department of Civil Engineering, California State Polytechnic University, USA

ABSTRACT

Seasonal floods occur predominantly in Tasmania at any time of the year (STORS, 2006). Improved streamflow predictability can be helpful for better Tasman seasonal flood forecasting and flood management in the rise of potential recent decade's climate change pattern. The present study focuses on evaluating the relationship between the Indo-Pacific Ocean and large continental ocean-atmospheric climate variability and with seven Tasmania river basins for around 42 years (1971~2012). The statistical technique named singular-valued decomposition (SVD) was applied on a standardized dataset for sea-surface temperatures (SST), 500mb geopotential height (Z_{500}) and 7 unimpaired Tasmanian river streamflow. The result identified the significant ocean-atmospheric regions (90% significance level) that influence hydrology of the Tasmanian rivers and subsequently lead to flood forecasts. SVD results showed that SST performed better seasonal variability in Tasman streamflow compared to Z_{500}, particularly during the winter season. But both the climate indices identify a significant southward trend region around the longitudes 175°W to 140°W and latitudes 25°S to 35°S which has better correlation with Tasman seasonal streamflow. This identified hypothesized region can be used as the probable driver of the Tasman basin streamflow. Understanding this correlation may provide better accuracy for long-lead river flood forecasting.

Keywords: Tasmanian rivers, climate indices, correlated regions, flood forecasting.

INTRODUCTION

Tasmania, an island state of Australia located southeast of the mainland (latitudes 40°S to 43.5°S and longitudes 144°E to 148°W) with an approximate area of 70000 square kilometers (Hill et al., 2009; Bobbie et al., 2013). The geographic presence of Tasmania causes warm summers and cold, wet winters (Bobbie et al., 2013), but the rainfall pattern of Tasmania is very much diversified as the highest rainfall is recorded during austral winter (June-July-August/JJA) and the lowest in summer (December-January-February/DJF). A recent study by CSIRO (2015) suggested that Tasmania will experience comparatively higher rainfall and subsequently higher streamflow during winter than average rainfall/streamflow trends of southern Australia. It indicates the impact of global climate change. Understanding the impact of climate variability on spatial and temporal characteristics of Tasmanian streamflow (TSF) will be helpful for better flood forecasting and risk assessment.

Establishing a relationship between climate variability and streamflow is always complex in nature as it is non-linear with respect to time and space (Sagarika et al., 2015). That's why hydrologists and climatologists around the world used various climate indices and drivers to correlate with streamflow pattern (Tootle and Piechota, 2006; Aziz et al., 2010; Lamb et al., 2010, Kalra et al., 2014; Sagarika et al., 2015). Among the climate drivers, Sea Surface Temperature (SST) has been most widely used for streamflow forecasting as it can remove bias from a particular spatial index (Tootle and Piechota, 2006). Additionally, Geopotential Heights (as 500-mbar geopotential height Z_{500}) is often used as a climate driver to understand the influence of atmospheric waves and improve forecast skill (Grantz et. 2005). Based on that, this study evaluates SST and Z_{500} against selected unimpaired streamflow gauges of Tasmania to identify the most influential correlated region that influences seasonal TSF pattern. Identification of significant ocean-atmospheric region will be useful for flood preparation.

APPROACH AND METHODS

DATA COLLECTION

In this study, 3 types of datasets have been used. These are unimpaired streamflow data of 7 Tasmanian gauges, gridded Sea Surface Temperature data (SST) of Indo-Pacific region and gridded 500-mbar Geopotential height data (Z_{500}). The descriptions of these data sets are provided below.

UNIMPAIRED TASMANIAN STREAMFLOW

Nowadays it is difficult to measure natural streamflow patterns as many rivers system have been diverted due to human intervention that alters channels. The Bureau of Meteorology (BoM), Australia usually maintains unimpaired streamflow stations data for Australian river-stream. These unimpaired stations are considered as free from anthropogenic interference. In this study, 12 unimpaired stations data were identified from the BoM Tasmanian region. Out of these stations, only seven unimpaired stations had long range and continuous monthly streamflow data set for over 42 years. Thus seven unimpaired stations of Tasmania were considered for 42 years (1971–2012). The spatial location of these stations is shown in Fig. 1. Streamflow data were analyzed based on the Tasman water year; i.e. 1 February to 31 January of the following year.

SEA SURFACE TEMPERATURE (SST) DATA

The monthly average Indo-Pacific SST data (version 4) were obtained from the NOAA ESRL Physical Sciences Division (https://www.esrl.noaa.gov/psd/data/gridded/data.noaa.ersst.v4.html). This is an open source data. The boundary of the SST data used in this study includes longitudes 30°E to

70°W and latitudes 60°S to 50°N for the entire study period (1971~2012). The SST data of NOAA is found in 2°×2° grid formation, and there are 7336 cells create for the whole study region. But, this study region contains lots of "land-mass" which were removed. Panoply (version 4.5.1), developed by Schmunk (2002), has been used to eliminate "land-mass" within the SST data. Panopoly is a product of the NASA Goddard Institute for Space Studies and is available for free (http://www.giss.nasa.gov/tools/panoply/). This data is standardized on each grid cell to remove the seasonality of the data.

GEOPOTENTIAL HEIGHT DATA

Similar to SST data, the monthly geopotential height (Z_{500}) mean index data is obtained from the NOAA Physical Sciences Center (http://www.esrl.noaa.gov/psd/data/gridded/data.ncep.reanalysis.derived.pressure.html) as open source in 2.5°×2.5° grid cell. The dataset is a production of the NCEP/NCAR Reanalysis project (Kalnay et al., 1996). The study boundary is identical to the SST study area which covers both land and ocean regions. The Z_{500} values are also standardized to reduce natural bias.

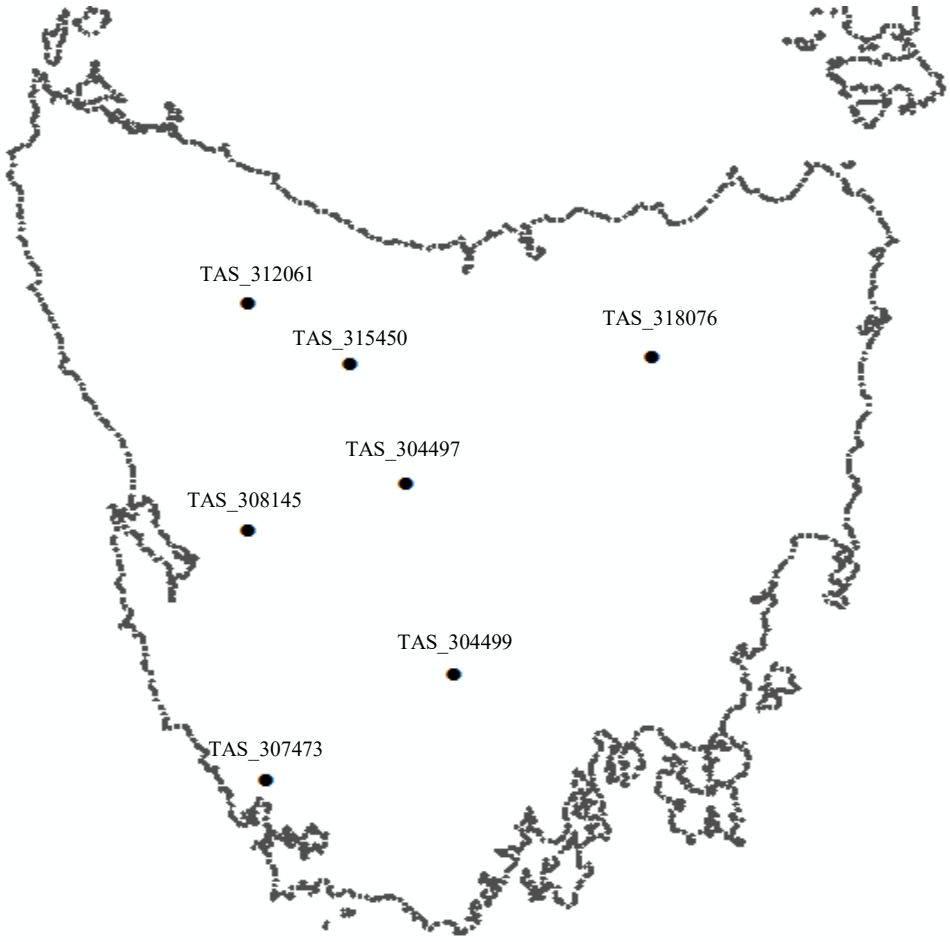

Figure 1: Locations of the 7 unimpaired Tasman streamflow reference stations (mentioned as BoM Id)

SINGULAR DECOMPOSITION METHOD (SVD)

The study evaluates the relationship between the TSF with seasonal (Summer/Dec~Feb, Autumn/Mar~May, Winter/July~Aug and Spring/Sep~Nov) climate drivers using statistical singular decomposition method (SVD). SVD is capable of identifying coupled relationships between two spatial-temporal fields (i.e. streamflow and climate drivers). Application of SVD has been extensive to climate-continental streamflow studies (Tootle and Piechota, 2006; Tootle et al. 2008; Aziz et al., 2010; Lamb et al., 2011; Oubeidillah et al., 2012; Kalra et al., 2014; Sagarika et al., 2015). Bretherton et al. (1992) and Strang (1998) provided a discussion of the SVD model. SVD uses an equal dimension of climate drivers' anomalies (SST/Z_{500}) and streamflow anomalies to compute a cross-variance matrix. The model also produces two orthogonal (which are called left and right orthogonal singular vector) and one diagonal matrix of singular values (e.g., orthogonal * diagonal * orthogonal) as shown in equation 1 (Strang, 1998).

$$SVD(_{COVER}TS) = \mathbf{U\Sigma V} \quad (1)$$

Where T represents the standardized climate data and S represents the streamflow (S) data fields. Both U and V represent the left and right singular (heterogeneous) matrices respectively, and **Σ** accounts for a non-zero diagonal matrix of singular values of the original matrix. Next, the model variabilities were measured by calculating the square covariance fraction (SCF) value of each mode as shown in equation 2.

$$\mathrm{SCF}_k = \frac{\mathrm{S}_\mathrm{k}^2}{\sum_i^r \mathrm{S}_\mathrm{i}^2} \quad (2)$$

In this equation, S represents the singular value at k-th mode. The singular values are ordered in ascending format (i.e. 1st mode is always greater than 2nd mode). This study considered only the mode that is greater or equal to an SCF of 10%. In the following step, temporal expansion series are computed by multiplying the first mode of U (or V) with the original T (or S) matrix. This generates the left temporal expansion series (LTES) a data vector.

$$LTES=\mathbf{U}'T' \quad (3)$$

Finally, the LTES is correlated with each grid cell in **S** and the RTES is correlated with each grid cell in **T** to compute the heterogeneous correlation (Uvo et al., 1998; Rajagopalan et al., 2000).

$$RTES=\mathbf{V}'S' \quad (4)$$

The values at 90% significance level are mapped (based on Pearson-r correlation coefficient) to display the influential regions of climate drivers (SST/Z_{500}) and TSF for different seasonal-time. Additionally, normalized square covariance (NSC) was calculated as shown in equation 5. Similar to SCF, NSC also identified the comparative measurement of SVD decomposition (Sagarika et al., 2015).

$$\mathrm{NSC} = \frac{\|\mathrm{C}\|_\mathrm{F}^2}{N_S * N_Z} \quad (5)$$

Where, $\|C\|_F^2$ is the sum of the squares of the singular values, N_s is the number of climate data points (SST and Z_{500}) and N_z is the number (7) of streamflow stations.

RESULTS

The sequence of SVD model input data (TSF and climate indices i.e. SST/Z_{500}) is shown in Table 1. The heterogeneous correlation maps for seasonal variability (Figs. 2) at 90% significant level are presented to identify the spatio-temporal relationships between TSF and climate drivers for the first mode. The blue color represents negatively correlated gauges/regions while red color shows positively correlated gauges/regions. Nonsignificant TSF stations are represented by black dots.

Table 1: Sequence of input data for SVD model (TSF and climate drivers)

Streamflow data for all analysis	F M A M J J A S O N D J	Standardized 12-months Total Streamflow Volume
Seasonal Analysis (Climate data SST/Z_{500})		
Summer All years 1971-2012	D J F	Standardized 3-months Avg. Climate Data
Autumn All years 1971-2012	M A M	Standardized 3-months Avg. Climate Data
Winter All years 1971-2012	J J A	Standardized 3-months Avg. Climate Data
Spring All years 1971-2012	S A N	Standardized 3-months Avg. Climate Data

TSF AND SEASONAL SST and Z_{500}

The climate drivers (SST and Z_{500}) and TSF seasonal analysis were performed using SVD for four seasons (summer: Dec-Feb; autumn: March-May; winter: June-Aug; spring: Sep-Nov).The summary of seasonal SVD results for SST and Z_{500} statistics with heterogeneous correlation maps are shown in Fig. 2 and Table 2 respectively. Table 2 represent the SCF value, significant cells numbers, correlation coefficient between expansion series of climate drivers, and NCF values. There was only one SCF mode obtained for each seasonal SVD analysis that varies 98% to 99%.

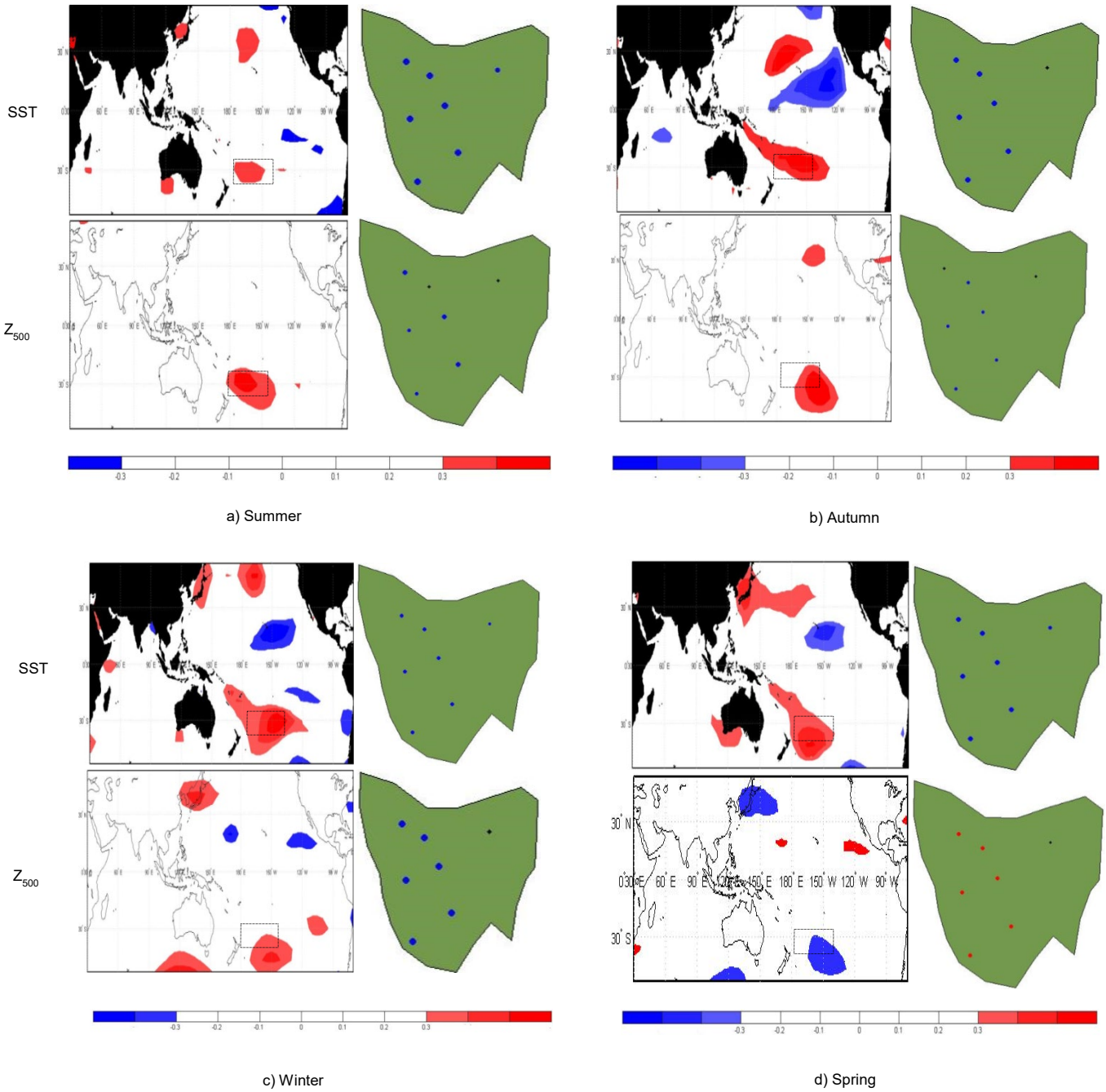

Figure 2: Heterogeneous correlation maps for a) summer: Dec-Feb; b) autumn: March-May; c) winter: June-Aug; d) spring: Sep-Nov; Correlations maps are produced at 90% significance level (red shows positive and blue shows negative correlations). The black boxed region showed the limits of the most common/persistent region.

This high SCF values indicated that there was not much variance within the two datasets and that the first mode was able to capture (or represent) almost all of the variances. It was also found that seasonal SST contained a higher number of significant grid cells compared to Z_{500}. Among them, the winter season showed a higher number of significantly correlated grids cells i.e. 1778 and 1243 respectively for SST and Z_{500} respectively. Similarly, it was obtained that, Pearson correlation value was the highest (0.36) for winter season between the spatio-temporal expansion series of SST-TSF. Again the highest variance of NSC values was obtained for the spring season for SST-TSF SVD analysis.

Table 2: Summary analysis of SVD model for TSF and climate drivers

Season	Squared Covariance Fraction SCF (%)		Significant cells		Correlation Coefficient |r| (between LTES & RTES)		Normalized Squared Covariance (NSC) Fraction (%)	
	SST	Z_{500}	SST	Z_{500}	SST	Z_{500}	SST	Z_{500}
Summer	98	98	1276	990	0.29	0.20	3.66	2.99
Autumn	99	98	1569	1020	0.32	0.21	3.85	3.03
Winter	99	99	1778	1243	0.36	0.30	3.52	3.74
Spring	99	98	1440	1148	0.32	0.29	4.33	3.32

The heterogeneous correlation maps for different seasons are shown in Fig 2a-2d. The results were calculated at 90% significance level. Fig. 2a displayed significantly correlated regions for both SST and Z_{500} with TSF during the summer season. Positively correlated regions (shown red) are found in the mid of north and south Pacific and the negatively correlated region (shown in blue) were detected near the equator of south Pacific (for SST-TSF analysis). But in the analysis of Z_{500}-TSF, it shows that only south Pacific region was positively correlated. In summer, all seven gauges showed significantly negative correlation with SST but five out of seven gauges showed a negative correlation with Z_{500}. Similarly, positively correlated regions were identified in the mid of north and south Pacific (for both SST-TSF and Z_{500}-TSF) and negatively correlated regions were found near north-equatorial Pacific (for only SST-TSF) during autumn season (Fig. 2b). In the winter season, major positive correlations were identified in south Pacific and north Pacific region near Japan (for both SST-TSF and Z_{500}-TSF). But the major negative correlations were identified near equatorial Pacific close to North-America. In this case, all seven stations were found negatively correlated with SST but six out of seven gauges showed negative correlations with Z_{500} in winter. In spring, the major positive correlations were identified for SST-TSF in south Pacific, north-Pacific along the coast of Japan and Western Australian coast. But the major negative correlations between Z_{500} and TSF were identified in south-Pacific and around Japanese coast. It is interesting to note that all seven stations showed negative correlation for SST-TSF SVD analysis while six out of seven stations showed positive correlation for Z_{500}-TSF SVD analysis.

Next, station-wise analyses were performed and correlation coefficients for different seasons are presented in Table 3. Analysis of data (Table 2) between climate drivers (SST and Z_{500}) and Table 3 established that Tasman rivers showed a higher percentage of correlation during the winter and spring season with the climate drivers. It indicated that dry season (summer and autumn) was less correlated with climate drivers than a wet season (winter and spring). The present study also showed that TAS stations located on the western coast of Tasmania are more reactive than northeastern station (TAS_318076) with seasonal climate drivers as here with SST and Z_{500} (Fig. 2).

Table 3: Correlation values |r| between temporal expansion series of TAS and SST/Z_{500}

Station ID	Correlation Coefficient |r|							
	SST				Z_{500}			
	Summer	Autumn	Winter	Spring	Summer	Autumn	Winter	Spring
TAS_304499	-0.46	-0.43	-0.54	-0.55	-0.49	-0.29	-0.58	0.60
TAS_312061	-0.52	-0.42	-0.55	-0.61	-0.57	-0.25	-0.60	0.63
TAS_318076	-0.36	-0.12	-0.26	-0.35	-0.14	0.04	-0.10	0.17
TAS_308145	-0.48	-0.55	-0.62	-0.54	-0.27	-0.36	-0.44	0.42
TAS_315450	-0.43	-0.49	-0.57	-0.50	-0.25	-0.33	-0.43	0.41
TAS_307473	-0.52	-0.54	-0.63	-0.56	-0.33	-0.37	-0.48	0.46
TAS_304497	-0.44	-0.45	-0.55	-0.54	-0.44	-0.29	-0.54	0.57

The results of the current study distinguished a common region around longitudes 175°W to 140°W and latitudes 25°S to 35°S which consistently showed correlation (positive/negative) with seasonal TSF (Fig. 2; black boxed regions).The persistency of this region may act as a potential climate index for the seasonal flow of Tasmanian rivers. In an earlier study by Kirono et al. (2010), NINO4 (5°N-5°S, 160°E-150°W; sea surface temperature (SST) in western Pacific), the Indonesian Index (II; SST over the Indonesian region) and some separate SST regions over Indo-Pacific may have the best potentiality for seasonal climate drivers for Australian streamflow. However, the current study identified that region around longitudes 175°W to 140°W and latitudes 25°S to 35°S may provide better forecast skill for seasonal TSF to act as a climate index. Although this study uses only 7 unimpaired river gauges of Tasmania, further research on this region is needed to better understand the physical explanation of the hydro-climactic teleconnection and improve the flood forecasting.

SUMMARY AND CONCLUSION

The current study focused on evaluating seasonal TSF by linking oceanic-atmospheric teleconnections to Tasmanian rivers for over 42 years (1971~2012). This long-term observation of seasonal TSF will be helpful for flood preparation of Tasmanian river basins. The identified coupled regions between SST, Z_{500} and TSF provides a comprehensive idea about the influences of climate variability on a broader spatial scale. Again, both SST and Z_{500} identified various significant ocean-atmospheric teleconnection regions that influence different hydrological regions of Tasmania. But most importantly, this study speculated a region around longitudes 175°W to 140°W and latitudes 25°S to 35°S which remained persistent and positively/negatively correlated with seasonal TSF. The persistent region may be helpful for regional flood planning and future flood management policy. It is true, this study has few limitations i.e. a small number of unimpaired gauges station and absence of longer instrumental data. The use of reconstructed tree ring for unimpaired gauges can potentially solve longer instrumental data problem (Carrier et al., 2013). Additionally, the inclusion of other climate drivers against the temporal extension series of TSF can provide new insights of the persistent region. Moreover, lag analysis up to several years can also check the survival limits of the persistent regions as climate indices for TSF at the current analysis. The authors acknowledged that some physical mechanisms for SST-TSF and Z_{500}-TSF are not well understood due to unexplained variances. Therefore, the new work should consider the hydro-climatology of this

persistent region for determining the more effective Tasmanian flood forecasting model. This will ensure better basin-wise hydrology estimates and enhanced flood preparation.

ACKNOWLEDGMENTS

This research is a part of a Ph.D. study at Curtin University of the first author under scholarship grant (Australia Postgraduate Award, Department of Education and Training, Australian Government). Authors also would like to thank Dr. Gnanathikkam Amirthanathan for supplying the streamflow data from Bureau of Meteorology, Australian Government.

References

Aziz, O., Tootle, G.,Gray, S., Piechota, T., (2010). Identification of Pacific Ocean sea surface temperature influences of Upper Colorado River Basin snowpack. Water Resources Research 46, W07536 (1-10). doi:10.1029/2009wr008053

Bobbi, C., Warfe, D., Hardie, S., (2013). IMPLEMENTING ENVIRONMENTAL FLOWS IN SEMI-REGULATED AND UNREGULATED RIVERS USING A FLEXIBLE FRAMEWORK: CASE STUDIES FROM TASMANIA, AUSTRALIA. River Research and Applications 30, 578-592. doi:10.1002/rra.2661.

Bretherton, C., Smith, C., Wallace, J., (1992). An Intercomparison of Methods for Finding Coupled Patterns in Climate Data. Journal of Climate 5, 541-560. doi:10.1175/1520-0442(1992)005<0541:aiomff>2.0.co;2

Carrier, C., Kalra, A., Ahmad, S., (2013). Using Paleo Reconstructions to Improve Streamflow Forecast Lead Time in the Western United States. JAWRA Journal of the American Water Resources Association 49, 1351-1366. doi:10.1111/jawr.12088

Commonwealth Scientific and Industrial Research Organization (CSIRO), (2015), “New climate change projections for Australia”, http://www.csiro.au/en/News/News-releases/2015/New-climate-change-projections-for-Australia (accessed 31 January 2017).

Grantz, K., Rajagopalan, B., Clark, M., Zagona, E., (2005). A technique for incorporating large-scale climate information in basin-scale ensemble streamflow forecasts. Water Resources Research 41, W10410. doi:10.1029/2004wr003467

Hill, K.,Santoso, A., England, M., (2009). Interannual Tasmanian Rainfall Variability Associated with Large-Scale Climate Modes. Journal of Climate 22, 4383-4397. doi:10.1175/2009jcli2769.1

Kalra, A., Sagarika, S., Ahmad, S., (2014). Investigation of the Linkages between Oceanic Atmospheric Variability and Continental U.S. Streamflow. In: World Environmental And Water Resources Congress 2014, American Society of Civil Engineers, Portland, Oregon, pp. 636-645.

Kalnay E, Kanamitsu M, Kistler R, Collins W, Deaven D, Gandin L,Woollen J. (1996). The NCEP/NCAR 40-year reanalysis project. Bull. Am. Meteorol. Soc. 77, 437–471.

Kirono, D., Chiew, F., Kent, D., (2010). Identification of best predictors for forecasting seasonal rainfall and runoff in Australia. Hydrological Processes 24, 1237–1247. doi:10.1002/hyp.7585

Lamb, K., Piechota, T., Aziz, O., Tootle, G., (2011). Basis for Extending Long-Term Streamflow Forecasts in the Colorado River Basin. Journal of Hydrologic Engineering 16, 1000-1008.

Oubeidillah, A., Tootle, G., Anderson, S., (2012). Atlantic Ocean sea-surface temperatures and regional streamflow variability in the Adour-Garonne basin, France. Hydrological Sciences Journal 57, 496-506. doi:10.1080/02626667.2012.659250

Rajagopalan, B., Cook, E., Lall, U., Ray, B., (2000). Spatiotemporal Variability of ENSO and SST Teleconnections to Summer Drought over the United States during the Twentieth Century. Journal of Climate 13, 4244-4255. doi:10.1175/1520-0442(2000)013<4244:svoeas>2.0.co;2

Sagarika, S., Kalra, A., Ahmad, S., (2015). Interconnections between oceanic–atmospheric indices and variability in the U.S. streamflow. Journal of Hydrology 525, 724-736. doi:10.1016/j.jhydrol.2015.04.020

STORS (2006). Floods & you: Tasmanian Flood Warning Consultative Committee (FWCC) community awareness project.

Strang, G. (1998). Introduction to linear algebra, 2nd Ed., Addison Wesley, Reading, Mass.

Tootle, G.Piechota, T., (2006). Relationships between Pacific and Atlantic ocean sea surface temperatures and U.S. streamflow variability. Water Resources Research 42, W07411 (1-14), doi: 10.1029/2005wr004184

Tootle, G., Piechota, T., Gutiérrez, F., (2008). The relationships between Pacific and Atlantic Ocean sea surface temperatures and Colombian streamflow variability. Journal of Hydrology 349, 268-276. doi:10.1016/j.jhydrol.2007.10.058

Uvo, C., Repelli, C., Zebiak, S., Kushnir, Y., (1998). The Relationships between Tropical Pacific and Atlantic SST and Northeast Brazil Monthly Precipitation. Journal of Climate 11, 551-562. doi:10.1175/1520-0442(1998)011<0551:trbtpa>2.0.co;2